Colloid Polym Sci 278:1211–1215 (2000)
© Springer-Verlag 2000

SHORT COMMUNICATION

K. Tanaka
Y. Oiwa
T. Kiguchi
R. Akiyama

Simultaneous optical observation of anisotropic texture for a concentrated solution of poly(γ-benzyl-L-glutamate) under transient stress response in shear flow

Received: 15 December 1999
Accepted: 12 July 2000

K. Tanaka (✉) · Y. Oiwa
T. Kiguchi · R. Akiyama
Department of Polymer
Science and Engineering,
Kyoto Institute of Technology,
Matsugasaki, Kyoto 606-8585, Japan
e-mail: ktanaka@ipc.kit.ac.jp

Abstract Simultaneous optical observation of anisotropic texture was performed under transient stress response in shear flow for a concentrated solution of poly(γ-benzyl-L-glutamate) (PBLG). Transient stress of the PBLG solution immediately after the onset of the shear flow showed a remarkable stress overshoot and damping oscillation behavior, followed by a steady state. On the other hand, simultaneous observation of the polarized optical microscopy showed the remarkable distortion of the banded texture immediately after the onset of the shear flow and the periodical changes in the retardation followed by a steady texture of the PBLG solution. The remarkable stress overshoot and the damping oscillation are closely related to the distortion of the banded texture and to the changes in the orientation of the rod-like molecules of the PBLG, respectively.

Key words Simultaneous optical observation · Polarized optical microscopy · Transient stress response · Poly(γ-benzyl-L-glutamate) · Liquid crystalline polymers

Introduction

Molecular orientation of liquid crystalline polymers is of great interest from the viewpoint of structural formation under external modulations of the deformation by the shear field, the electric field, the magnetic field, and so on. It is well known that liquid crystalline polymers composed of rod-like molecules show the instability after the stepwise changes in the shear rate [1]. For instance, transient stress after the onset of the shear flow shows a stress overshoot and damping oscillation behavior. Then the stress reaches a steady state. It is thought that the flow instability is closely related to the fact that the director, the unit vector with the average direction of orientation of the rod-like molecules, cannot be determined (or fixed) even under shear flow. As shown in Fig. 1, the Miesowicz viscosities are defined for the three cases of the fixed director of rod-like molecules [2]. Because the director is parallel to the velocity gradient in the case of η_c, the flow resistance of the molecules, which is proportional to the stress at a constant shear rate, is the largest. However, the flow resistance is much smaller in the case of η_b because the director is parallel to the flow direction. The director is forced to rotate by the hydrodynamic torque in a simple shear flow, which is referred to as the director tumbling. Further, it is well known that the monodomain texture is difficult to find but the polydomain texture is usually found by the polarized optical microscopy even for the sheared samples of liquid crystalline polymers [3]. This is entirely different from the case of low molecular weight liquid crystals, and a mesoscopic theory of the director tumbling in the polydomain texture successfully simulates the features of the rheological behavior, including the oscillation of the stress [4]. In addition, the authors are interested in the rheological behavior of liquid crystalline polymers under external modulation of the

---

Supplementary material for this paper (Fig. 5–7 in color oder so) can be obtained electronically by using the Springer LINK server located at http://link.springer.de/link/service/journals/00396/index.htm

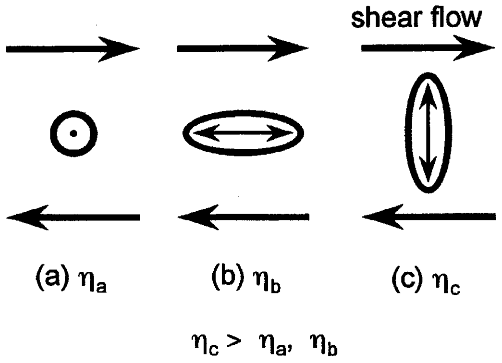

Fig. 1a–c Miesowicz viscosities: **a** director perpendicular to flow direction and to velocity gradient; **b** director parallel to flow direction; **c** director parallel to velocity gradient ($\eta_c > \eta_a, \eta_b$)

electric field, the electro-rheological (ER) effect. The complex behavior of the polydomain texture would also be induced by the external modulation of the electric field under shear deformation. Within each domain in the polydomain texture, the director can also be determined, the "local" director, and the "local" dielectric constant is usually anisotropic. The domain would also be deformed by the external electric field. Therefore, the ER effect of liquid crystalline polymers is related to the orientation and interaction of the domains in the polydomain texture not only under an external electric field but also under shear flow [5]. The investigation on the flow behavior under no electric field also provides us with helpful pieces of information for understanding the ER effect of liquid crystalline polymers. It is not too much to say that the complex rheological behavior is related to the complex behavior of the polydomain texture under shear flow, after cessation of the shear flow, as well as under external modulation of the electric (or magnetic) field.

On the other hand, there are some experiments to reveal the complex behavior of the polydomain texture by optical methods such as flow birefringence measurement [6], spectrographic birefringence techniques [7, 8], in-situ X-ray and small angle neutron scattering measurements [9, 10], and also optical observation [3, 11]. However, the complex behavior of the polydomain texture has not yet been fully understood. There are only a few reports on optical observation under shear flow, still less than optical observation simultaneously performed with rheological measurement. Optical observation provides directly data on the global and local behavior of the polydomain texture, which is a useful method to understand the complexity of the behavior. (Methods involving other than optical observations are also useful, of course, but the results obtained are the average of the complex behavior. The spatial distribution of the polydomain texture is effectively obtained by optical observation.) In the present paper, simultaneous optical observation of anisotropic texture is performed under transient stress response in shear flow for a concentrated solution of poly(γ-benzyl-L-glutamate) (PBLG). The transient stress response from immediately to sufficiently after the onset of the shear flow is discussed in terms of the behavior of anisotropic texture observed simultaneously.

Experimental

Solution of poly(γ-benzyl-L-glutamate) (PBLG) was used in the present study. The PBLG with the average molecular weight based on viscosity of 2.96×10^5 was purchased from Sigma Chemical Co. The PBLG as received was dissolved in 1,4-dioxane. The concentration of the PBLG was 15 wt%, and the solution was found to be anisotropic at the concentration and room temperature from the optical observation.

Transient stress response after the onset of the shear deformation was measured using a rotational rheometer with a fixture of parallel plates [5]. The fixture was made of glass covered with a conducting layer of tin oxides. The diameter of the glass plates was 40 mm, and the gap between the glass plates was 0.1 mm. The gap was adjusted by a micrometer attached to the rheometer, and the gap of zero was determined by the electrical conduction of the two glass plates with the conducting layer. The shear rate at the edge of the parallel plates was 2.6 s^{-1}. (It should be noted that the shear rate is proportional to the distance along the radial direction from the center of the disk.) The behavior of anisotropic texture was also observed simultaneously with the rheometer equipped with a polarized optical microscope with crossed polarizers as shown in Fig. 2.

Results and discussion

Observed color of transmitted light

In our optical observation system, the sample solution is placed between a polarizer and analyzer of which axes cross one another and at an angle of $\psi = \pi/4$ (rad) with

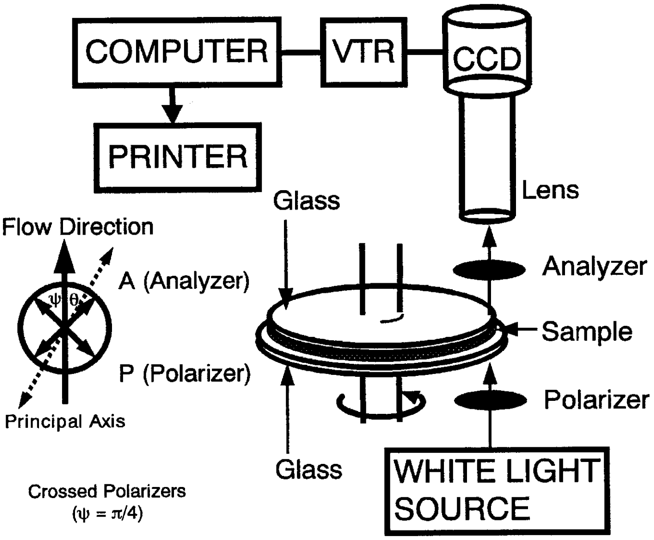

Fig. 2 Schematic illustration of the simultaneous optical observation system with the rheological measurements

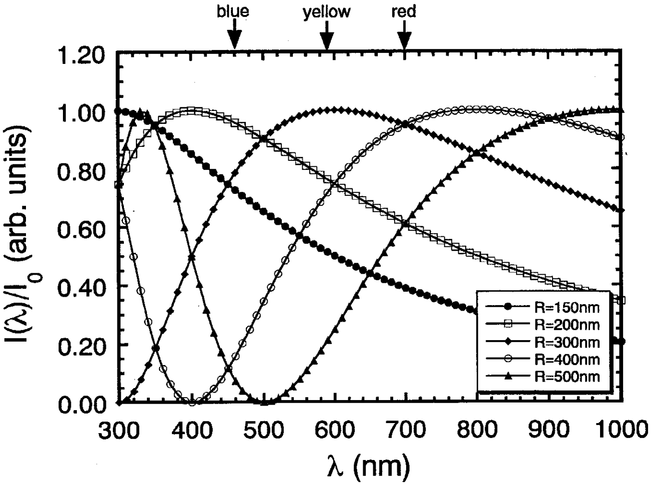

Fig. 3 Calculated spectra of the transmitted light using Eq. (1) and typical values of the retardation (R), where no attenuation of light and $\theta = 0$ are assumed

respect to the flow direction. Assuming that a sample with birefringence Δn is oriented with its principal axis at an angle θ as shown in Fig. 2, the transmitted intensity of light with the wavelength λ, $I(\lambda)$, is expressed as the following equation [7]:

$$I(\lambda)/I_0 = \exp(-2\alpha'') \sin^2(\pi R/\lambda) \cos^2(2\theta)/2 \qquad (1)$$

where

$$R = \Delta n\, d \qquad (2)$$

In Eq. (1), the term $\exp(-2\alpha'')$ accounts for attenuation of light, I_0 is the intensity of incident light, R is the retardation of the sample, and d is the sample thickness. For the discussion of the wavelength dependence of the transmitted light intensity, let α'' and θ be constant. Then the term $\sin^2(\pi R/\lambda)$ is responsible for the wavelength dependence in Eq. (1). Figure 3 shows the wavelength dependencies of the transmitted light intensity in arbitrary units. In the calculation of Eq. (1), the retardation is assumed to be from 150 nm to 500 nm because the birefringence of the uniaxially aligned monodomain solution of PBLG, which is of similar molecular weight and concentration to ours, with molecular orientation parallel to the glass surface and $\theta = 0$ is reported to be around 0.006 [7]. In the present study, white light is used as the incident light. Therefore, the color of the transmitted light is determined by spectrum as shown in Fig. 3, depending on the retardation of the sample. In Fig. 3, the wavelength of the maximum intensity in a spectrum, λ_{max}, becomes longer (the red shift), as the retardation increases, up to 300 nm. Another peak at the ultra-violet region is found in a spectrum for R = 400 nm and 500 nm. It can be thought qualitative that the visible color of the transmitted light shifts blue to red as the retardation increases, except for the limiting retardation of our sample. However, it cannot be denied that the retardation of our sample changes in the range larger than 600 nm. Even then, similar changes in the color sequence of the transmitted light, the red shift, is also obtained by the calculation in Eq. (1). Therefore, the red shift can be qualitatively related to the increase in the retardation of the sample.

Transient stress response after the onset of the shear flow

Figure 4 shows a transient stress response after the onset of the shear flow. Before the onset of the shear flow, the sample was sheared and relaxed sufficiently. Therefore, the banded texture with bands aligned perpendicular to the flow direction [3] was developed, as shown in Fig. 5a, before the rheological measurement. Further, the optical observation was performed simultaneously with the rheological measurement. In Fig. 4, the arrow with "5a" indicates the time at which the micrograph shown in Fig. 5a was recorded, for instance. The transient stress immediately after the onset of the shear flow shows a remarkable stress overshoot and damping oscillation behavior. Then the stress reaches a steady state. This behavior, shown in Fig. 4, is qualitatively consistent with the behavior reported previously [1, 8]. However, the initial texture of the PBLG solution in the present experiment, the banded texture, was considerably different from the texture reported so far. For instance, the homeotropic orientation, in which the PBLG molecules were oriented perpendicular to the glass surface, or the parallel orientation to the glass surface, was initially prepared in the start-up flow experiment [11]. The polydomain texture, in which anisotropic domains were randomly distributed, was

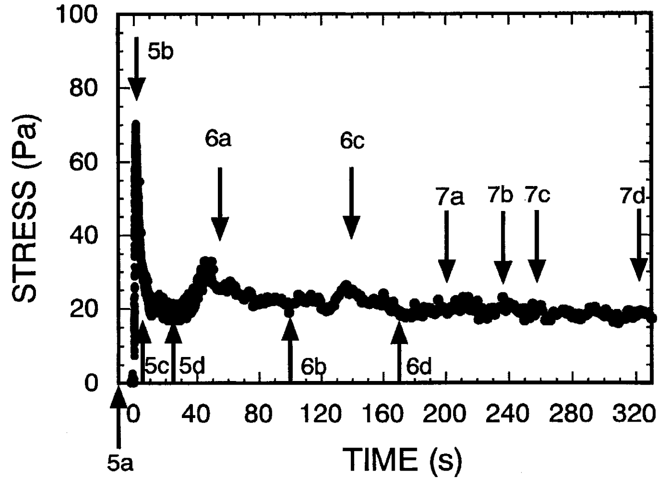

Fig. 4 Transient stress response after the onset of the shear flow. The arrows indicate the times at which the micrographs in the following figures were recorded. For instance, the arrow with "5a" indicates the time at which the micrograph of Fig. 5a was recorded

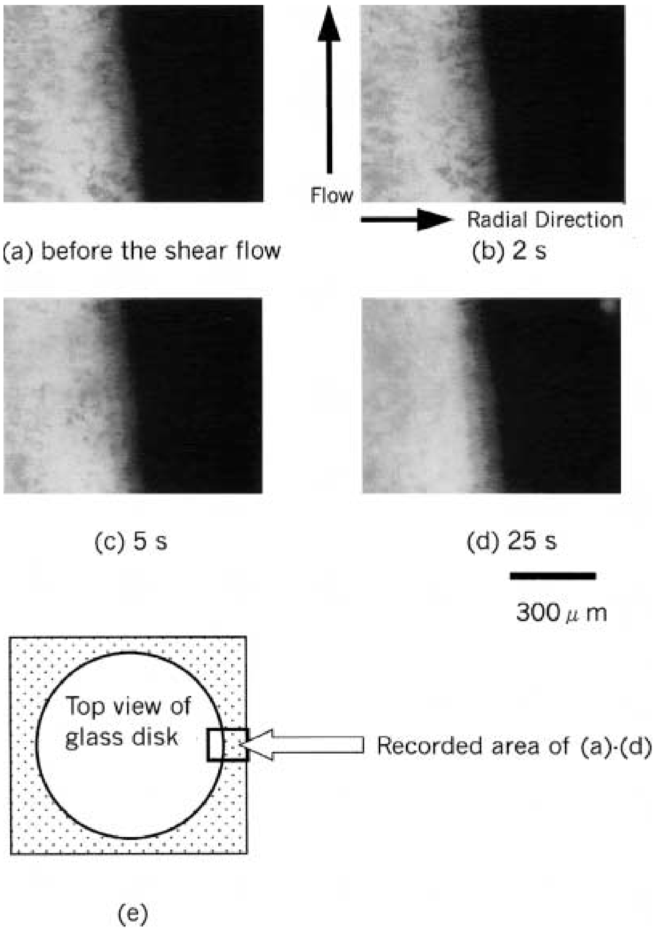

Fig. 5a–e Polarized optical micrographs of the PBLG solution simultaneously observed before and immediately after the onset of the shear flow

also initially produced in the stepwise changes in the shear rate [1, 8]. The difference in the initially prepared texture would affect the initial behavior of the stress overshoot in the present study.

Simultaneous observation after the onset of the shear flow

Figure 5 shows the polarized optical micrographs of the PBLG solution simultaneously observed before and immediately after the onset of the shear flow. In the figure, the flow and radial direction of the glass disk is shown by arrows, and the interface between colored area and dark area is the edge of the upper glass disk. That is, there were no PBLG molecules in the dark area. In the figure, the banded texture developed before the shear flow, Fig. 5a, is remarkably distorted (Fig. 5b–d) and the color is changed from blue to orange. Further, the polydomain texture composed of small anisotropic grain-like domains in colored area can be found in Fig. 5c, d.

Figure 6 shows the polarized optical micrographs of the PBLG solution successively after the observation in Fig. 5. As mentioned in the experimental section, the shear rate is proportional to the distance along the radial direction from the center of the disk. Therefore, the shear rate is highest at the edge of the parallel plates, and our attention will be mainly focused on the behavior of the edge texture. (For the results obtained by the parallel-plate rotational rheometer, the shear rate at the edge is generally discussed as a characteristic shear rate. The PBLG molecules would be effectively deformed at the edge because of the maximum shear rate. However, the torque element acting on the inner region of the glass disk cannot be neglected. The homogeneous distribution of the shear rate can be obtained by the use of a fixture of cone and plate or a sliding rheometer with parallel plates.) In Fig. 6, the color of the edge texture changes periodically, which corresponds to the periodical changes in the retardation. The color of edge textures in Fig. 6a, c is blue, while the color in Fig. 6b, d is orange. As discussed in the previous section, $\lambda_{\max}$ in Fig. 3 showed the red shift as the retardation increases. Then, the PBLG molecules or helixes, the axes of which are principle axes, tend to orientate parallel to the flow direction. On the other hand, the transient stress response observed simultaneously shows a damping oscillation behavior indicated by the corresponding arrows in Fig. 4. Accordingly, the PBLG molecules tend to orientate perpendicular to the glass surface at the

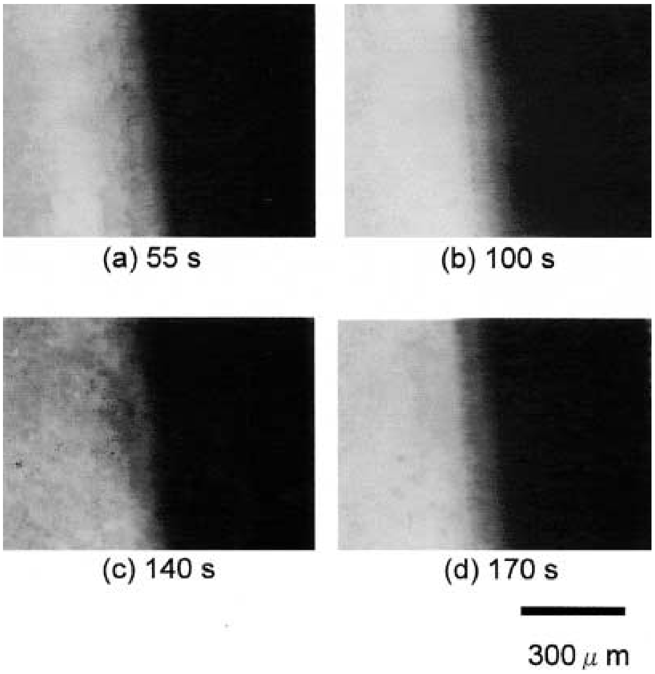

Fig. 6a–d Polarized optical micrographs of the PBLG solution simultaneously observed after the onset of the shear flow

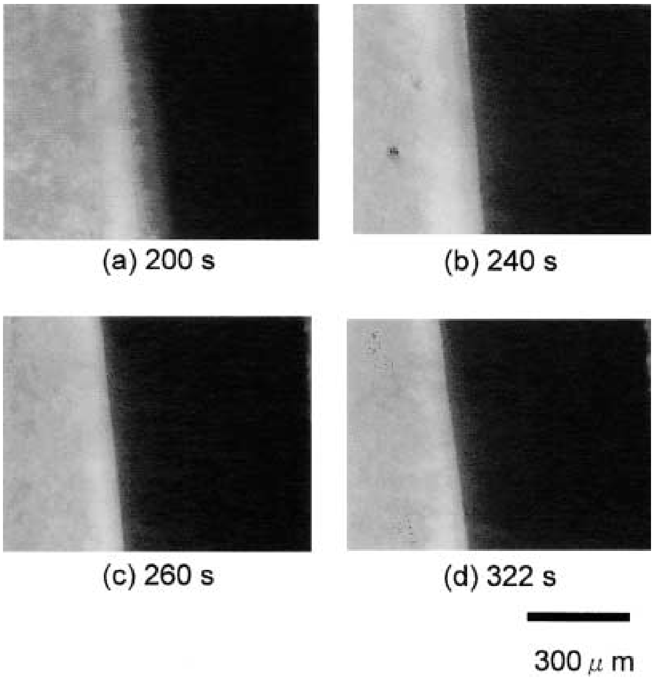

(a) 200 s (b) 240 s

(c) 260 s (d) 322 s

Fig. 7a–d Polarized optical micrographs of the PBLG solution simultaneously observed sufficiently after the onset of the shear flow

peak in the stress response (around the arrows with 6a and 6c in Fig. 4), while the molecules tend to orient parallel to the glass surface at the bottom of the stress response (around the arrows with 6b and 6d in Fig. 4). Of course, the molecules are distributed in the three-dimensional space. The molecular orientation to the flow direction projected on the glass plane, which correlates with the angel θ, would be changed at the same time as the shearing time increases. It is also thought that the PBLG molecules tend to align parallel to the flow direction with the changes in the absolute value of the angle θ ranging from 0 to $\pi/2$.

Figure 7 shows the polarized optical micrographs of the PBLG solution observed sufficiently after the onset of the shear flow. In the figure, the texture of the PBLG solution is relatively steady. In particular, the color of the edge texture shown in Fig. 7d is orange (or red), which shows the parallel orientation to the glass surface of the PBLG molecules is the higher and steadier. The molecular orientation to the flow direction projected on the glass plane would also be the higher and steadier. On the other hand, the color changes along the radial direction. It is seen that the color in Fig. 7b distributes blue, yellow, and red in order. Qualitatively, this order of color distribution corresponds to the red shift of $\lambda_{\max}$ in Fig. 3. The degree of the parallel orientation to the glass surface of the PBLG molecules can be distributed along the radial direction. As shown in Fig. 7, however, the color in Fig. 7d distributes discontinuously although the shear rate is proportional to the distance from the center of the disk. That is, the retardation changes abruptly in the outer region of the glass disk, and a part of the (orange) concentric ring on the glass disk, at which the molecular orientation would be relatively high, is seen in the region. It is thought that the PBLG molecules at the edge, which were deformed at the maximum shear rate, were first oriented and the orientation affects the molecules in the vicinity of the edge. The polydomain texture could be found in the outer region as well as in the inner region of the glass disk although further observation with much higher magnification would be required to discuss the texture more precisely. In addition, direct information for the ER effect of liquid crystalline polymers would be obtained by the observation of the texture under external modulation of the electric field. Observation under the electric field will be performed in the near future.

Conclusions

An optical observation system to be used simultaneously with rheological measurements was constructed and observations were carried out which are reported in the present paper. The remarkable stress overshoot and the damping oscillation were found in the transient stress response after the onset of shear flow. Simultaneous observation by means of polarized optical microscopy showed that the remarkable stress overshoot and the damping oscillation are closely related to the distortion of the banded texture and to the periodical changes in the orientation of the PBLG molecules, respectively.

References

1. Moldenaers P, Fuller G, Mewis J (1989) Macromolecules 22:960
2. de Gennes PG, Prost J (1993) The physics of liquid crystals, 2nd edn. Oxford University Press, New York, chap 5
3. Kiss G, Porter RS (1980) Mol Cryst Liq Cryst 60:267
4. Larson RG, Doi M (1991) J Rheol 35: 539
5. Tanaka K, Takahashi A, Akiyama R, Kuramoto N (1999) Phys Rev E 59: 5693
6. Asada T, Muramatsu H, Watanabe R, Onogi S (1980) Macromolecules 13: 867
7. Hongladarom K, Burghardt WR, Baek SG, Cementwala S, Magda JJ (1993) Macromolecules 26:772
8. Hongladarom K, Burghardt WR (1993) Macromolecules 26:785
9. Walker LM, Wagner NJ (1996) Macromolecules 29:2298
10. Hongladarom K, Ugaz VM, Cinader DK, Burghardt WR, Quintana JP, Hsiao BS, Dadmun MD, Hamilton WA, Butler PD (1996) Macromolecules 29:5346
11. Larson RG, Mead DW (1992) Liq Cryst 12:751